A Series of Molybdenum(V) Complexes with the Oxalato Ligand Engaged in Different Binding Roles − An Unusual Staggered Conformation of the μ_4-Oxalate in $[\{Mo_2O_4(\eta^2\text{-}C_2O_4)_2\}_2(\mu_4\text{-}C_2O_4)]^{6-}$

Barbara Modec,*[a] Jurij V. Brenčič,[a] and Jože Koller[a]

Keywords: Coordination modes / Molybdenum / Oxo ligands / Oxalate / Polyoxometalates

Solvothermal reactions between mononuclear halooxomolybdates(V) and oxalic acid afforded smaller oligonuclear complexes with the oxalate ion engaged in different binding modes. The oxalate ion coordinates as a bidentate terminal ligand to each metal centre of the $\{Mo_2O_4\}^{2+}$ unit to form the anion of $(MeNC_5H_5)_2[Mo_2O_4(\eta^2\text{-}C_2O_4)_2py_2]$ (**1**; py = pyridine; $MeNC_5H_5^+$ = *N*-methylpyridinium cation). $(MeNC_5H_5)_6[\{Mo_2O_4(\eta^2\text{-}C_2O_4)_2\}_2(\mu_4\text{-}C_2O_4)]$ (**2**) with a tetradentate oxalate ion connecting two dinuclear subunits is a very rare example of a coordination compound with the oxalato ligand in a completely staggered conformation: the two CO_2 entities of the μ_4-oxalate ion are rotated by 90° with respect to each other. Ab initio MO calculations on $[\{Mo_2O_4(\eta^2\text{-}C_2O_4)_2\}_2(\mu_4\text{-}C_2O_4)]^{6-}$ revealed the isomer with the staggered conformation of the μ_4-oxalate ion to be of the lowest energy. The cyclic octanuclear anion of $(MeNC_5H_5)_2[Mo_8O_{16}(OMe)_8(\mu_8\text{-}C_2O_4)]$ (**3**) consists of four dinuclear subunits arranged around the central oxalate ion and additionally linked by pairs of methoxide bridges. Each oxygen atom of the oxalate ion bridges a pair of metal centres not connected by a metal–metal bond. The anionic part of $[MeNC_5H_2(Me)_3]_2[HNC_5H_2(Me)_3]_2[Mo_2O_3(\eta^2\text{-}C_2O_4)_4]$ (**4**) [$MeNC_5H_2(Me)_3^+$ = *N*-methylcollidinium cation; $HNC_5H_2(Me)_3^+$ = protonated 2,4,6-collidine] possesses an *anti*-$\{Mo_2O_3\}^{4+}$ structural fragment with a pair of bidentate oxalate ions coordinated to each molybdenum atom. The compounds were fully characterized by X-ray structural analysis and infrared spectroscopy.

Introduction

The continuous interest in polyoxometalates, in particular those with incorporated organic groups, is driven by their structural analogy to metal oxide surfaces, their use as models for the catalytic reactions taking place at these surfaces and also by the search for novel materials, distinguished by special structural and magnetic properties.[1] The mechanism of their formation is still not well understood. Mostly it is described as the self-assembly of known species. The basic building unit in the chemistry of molybdenum in the +5 oxidation state is a particularly stable dinuclear fragment, shown in Scheme 1 and henceforth symbolised by $\{Mo_2O_4\}^{2+}$. Its two d^1 metal centres are bridged by a pair of oxygen atoms. A single metal−metal bond with the usual length in the 2.5−2.6 Å range participates in the cohesion of the unit.[2] A set number of available coordination sites allows coordination of numerous ligands, while in their absence further aggregation takes place and larger, more stable assemblies are formed. The X-ray structure analyses of many $\{Mo_2O_4\}^{2+}$ compounds have shown that the structural integrity of the dinuclear unit remains intact irrespective of the nature of ligands completing the immediate environment of the metal atom.[2] Among the very diverse ligands which fulfil molybdenum's coordination demands, multidentate oxygen donor ligands have been used with the aim of assisting in the linkage of dinuclear blocks into polymeric materials. With only a few exceptions, the self-assembly process of dinuclear fragments prevailed, leading to discrete cluster species with the multidentate ligands incorporated into the metal oxide cores. As shown with some examples from the recent literature, various typical patterns of assembly can be recognized. For instance, the hexanuclear motif in $[(Mo_2O_4)_3(\mu_6\text{-}AsO_3)(\mu_2\text{-}SO_4)_3(\mu_2\text{-}OH)_3]^{6-}$,[3] $[(Mo_2O_4)_3(\mu_6\text{-}CO_3)(\mu_2\text{-}CO_3)_3(\mu_2\text{-}OH)_3]^{5-}$,[4] and $[(Mo_2O_4)_3(\mu_6\text{-}SO_3)(\mu_2\text{-}SO_3)_3(\mu_2\text{-}O)_3]^{8-}$,[5] is the same as first observed among the phosphomolybdates(V):[6] three $\{Mo_2O_4\}^{2+}$ building blocks are arranged around the central μ_6-bridging ligand [arsenate(III),[3] carbonate,[4] sulfate(IV)[5] or phosphate[6]] to form a planar hexanuclear moiety with three μ_2-bridging ligands [sulfate,[3] carbonate,[4] sulfate(IV)[5] or phosphate[6]] on its periphery. These hexanuclear moieties tend to aggregate even further: in

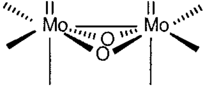

Scheme 1. $\{Mo_2O_4\}^{2+}$ structural unit

---

[a] Faculty of Chemistry and Chemical Technology, University of Ljubljana,
Askerčeva 5, 1000 Ljubljana, Slovenia
Fax: (internat.) + 386-1/2419-220
E-mail: barbara.modec@guest.arnes.si

DOI: 10.1002/ejic.200300741

$\{Mn^{II}[P_4Mo_6O_{28}(OH)_3]_2\}^{16-}$ and $\{Co^{II}[P_4Mo_6O_{28}(OH)_3]_2\}^{16-}$,[7] two recent examples of the basic hexanuclear motif with bridging phosphate ions, the transition metal cation is sandwiched between two hexanuclear moieties to form a "dimer". These "dimers" are linked further through strong ionic interactions into polymeric materials. However, the mixed-valent $[(Mo_2O_4)_3(Mo^{VI}O_4)(O_3PCH_2PO_3)_3]^{8-}$ reveals a new pattern of assembly.[8] Rather than sharing edges as in the above-described examples, three pairs of octahedra arranged around the central molybdate(VI) share corners. Apparently, the larger size of the μ_6-bridging ligand, molybdate(VI) vs. phosphate, arsenate(III) etc., induces the change in the connectivity between the $\{Mo_2O_4\}^{2+}$ blocks. The sulfate(IV) ion has also been seen to connect six $\{Mo_2O_4\}^{2+}$ units into a bulky $[(Mo_2O_4)_6(\mu_2\text{-}SO_3)_{12}(\mu_3\text{-}SO_3)_4]^{20-}$ core.[5] Its structure resembles that of an ε-Keggin derivative.[9] Another example, $[(Mo_2O_4)_{10}(P_2O_7)_{10}(CH_3COO)_8(H_2O)_4]^{28-}$, with coordinated pyrophosphate and acetate ions features an even larger assembly of dinuclear blocks.[10] These are arranged into two groups, one of six and the other of four dinuclear blocks to form two non-equivalent interconnected rings.

In only three cases does the interaction between the $\{Mo_2O_4\}^{2+}$ unit and the multidentate ligand result in a true polymeric material: (i) $[Mo_2O_4(PO_4)(HPO_4)]_n^{3n-}$ with $\{Mo_2O_4\}^{2+}$ units linked in a complicated manner by bridging phosphate ions into a two-dimensional array;[11] (ii) $[Mo_2O_4(C_2O_4)_2(H_2PO_4)]_n^{3n-}$ where μ_2-phosphate ions link dinuclear units into polymeric chains;[12] and (iii) $[Mo_2O_4(\mu_2\text{-}C_2O_4)Cl_2]_n^{2n-}$, prepared in our laboratory, which has infinite chains containing alternating $\{Mo_2O_4\}^{2+}$ units and bis(bidentate) oxalate ions.[13] Our choice of the oxalate ion among many oxygen donor ligands was governed by its ability to adopt several coordination modes. The binding mode the ligand eventually adopts depends, to a certain extent, upon the ratio between the ligand and the central atom. Studies of the interaction between the oxalate ion and the molybdenum(V) starting material resulted, apart from the polymeric $[Mo_2O_4(\mu_2\text{-}C_2O_4)Cl_2]_n^{2n-}$, in a series of smaller $\{Mo_2O_4\}^{2+}$ assemblies. We report herein on the syntheses and the characterization of $(MeNC_5H_5)_2[Mo_2O_4(\eta^2\text{-}C_2O_4)_2py_2]$ (**1**), $(MeNC_5H_5)_6[\{Mo_2O_4(\eta^2\text{-}C_2O_4)_2\}_2(\mu_4\text{-}C_2O_4)]$ (**2**), $(MeNC_5H_5)_2[Mo_8O_{16}(OMe)_8(\mu_8\text{-}C_2O_4)]$ (**3**) and $[MeNC_5H_2(Me)_3]_2[HNC_5H_2(Me)_3]_2[Mo_2O_3(\eta^2\text{-}C_2O_4)_4]$ (**4**).

Results and Discussion

Structural Studies

Crystal Structure of $(MeNC_5H_5)_2[Mo_2O_4(\eta^2\text{-}C_2O_4)_2py_2]$ (1)

The crystal structure of **1** consists of $[Mo_2O_4(\eta^2\text{-}C_2O_4)_2py_2]^{2-}$ anions (Figure 1) and *N*-methylpyridinium cations. Selected bond lengths are given in Table 1. Two molybdenum atoms are bridged by a pair of oxygen atoms to form the $\{Mo_2O_4\}^{2+}$ structural moiety. Its geometry follows a well-established pattern.[2] The distance between

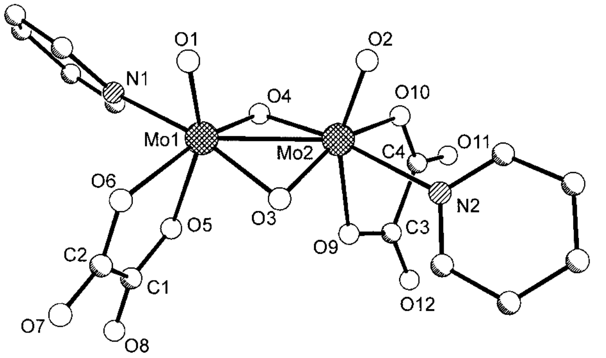

Figure 1. Drawing of $[Mo_2O_4(\eta^2\text{-}C_2O_4)_2py_2]^{2-}$, the anionic part of **1**, showing the atom labelling scheme; molybdenum atoms are cross-hatched; nitrogen atoms are lined bottom left to top right, oxygen atoms are unshaded and carbon atoms shaded, small-sized spheres; the same drawing scheme applies to all figures

Table 1. Selected bond lengths [Å] for **1**

Mo(1)−O(1)	1.690(2)	Mo(2)−O(2)	1.690(2)
Mo(1)−O(3)	1.944(2)	Mo(2)−O(3)	1.927(2)
Mo(1)−O(4)	1.932(2)	Mo(2)−O(4)	1.944(2)
Mo(1)−O(5)	2.179(2)	Mo(2)−O(9)	2.157(2)
Mo(1)−O(6)	2.120(2)	Mo(2)−O(10)	2.135(3)
Mo(1)−N(1)	2.260(3)	Mo(2)−N(2)	2.268(3)
Mo(1)−Mo(2)	2.5468(4)		

Table 2. Selected geometric parameters [Å, °] of the $\{Mo_2O_4\}^{2+}$ unit in some compounds

	Mo−Mo	Fold angle	O_b−Mo−O_b [a]	Mo−O_b−Mo
1	2.5468(4)	149.62(6)	94.02(10), 94.18(10)	82.16(9), 82.29(9)
2	2.5655(4)	160.21(5)	95.73(7)	82.73(7)
3	2.5770(4), 2.5786(4)	156.43(14), 156.83(18)	93.89(9)−94.47(9)	83.30(8)−83.94(8)
$[Mo_2O_4Cl_2(4\text{-}EtPy)_4]$[14] [b]	2.5489(5)	144.51(14)	92.3(1), 92.5(1)	82.29(9), 82.7(1)
$(PyH)_2[Mo_4O_8(OEt)_2(HOEt)_2Br_4]$[15] [c]	2.6060(4)	152.22(12)	93.61(8), 93.71(9)	82.09(8), 84.39(8)
$(Et_3NH)[Mo_6O_{12}(OMe)_4(acac)_3]$[16] [d]	2.595(1)−2.608(1)	152.6[e]	94−95[e]	80−85[e]
$(MeNC_5H_5)_{2n}[Mo_2O_4(C_2O_4)Cl_2]_n$ [13]	2.5607(7)	150.21(8)	93.31(10)	83.10(9)
$(3\text{-}MePyH)_{2n}[Mo_2O_4(C_2O_4)Cl_2]_n$ [13]	2.5832(4)	148.77(6)	92.84(7)	83.20(6)

[a] O_b denotes bridging oxygen atoms in the $\{Mo_2O_4\}^{2+}$ unit. [b] A neutral dinuclear compound. [c] Contains a tetranuclear anion built up from two $\{Mo_2O_4\}^{2+}$ units. [d] acac = acetylacetonate. Contains a hexanuclear anion with three $\{Mo_2O_4\}^{2+}$ units arranged around the central methoxide unit. [e] The angles were calculated from data of the CCDC.[17]

molybdenum atoms, 2.5468(4) Å, is shorter than those observed in larger $\{Mo_2O_4\}^{2+}$ assemblies (see Table 2). The $Mo(O_b)_2Mo$ ring is not planar, instead it is folded about the line connecting the bridging oxygen atoms (O_b). The dihedral angle between two $Mo(O_b)_2$ planes, commonly denoted as the fold angle,[2] is 149.62(6)°. The six-coordination of each molybdenum atom is completed with a bidentate oxalate ion and a pyridine ligand.

Dinuclear oxalato complexes of molybdenum(V) have been studied before.[18] Their dinuclear nature, initially formulated on the basis of spectroscopic data and diamagnetism, was first confirmed by the X-ray structure analysis of $Ba[Mo_2O_4(\eta^2\text{-}C_2O_4)_2(H_2O)_2]\cdot 3H_2O$,[19] which was also the first crystal structure of an $\{Mo_2O_4\}^{2+}$-containing compound. The literature also mentions the $[Mo_2O_4(C_2O_4)_2py_2]^{2-}$ species, although no X-ray structural data were given to support its formulation.[20] In $Ba[Mo_2O_4(\eta^2\text{-}C_2O_4)_2(H_2O)_2]\cdot 3H_2O$,[19] in contrast to the well-documented and uniform tendency of Mo=O bonds to weaken bonds *trans* to themselves, no significant *trans* influence was observed. The molybdenum-to-oxalato-oxygen bond length *trans* to the oxo ligand is 2.14(4) Å compared to 2.11(3) Å for the same bond in the *cis* position. The earlier belief that the oxalato ligand has a low *trans* susceptibility compared to other ligands[21] was ruled out by the later structural determinations of a series of compounds containing the $[Mo_2O_4(\eta^2\text{-}C_2O_4)_2(H_2O)_2]^{2-}$ anion, which clearly indicated the existence of a *trans* influence.[22] However, the effect was not equally conspicuous in all these compounds. In the anion of **1**, two sets of non-equivalent bond lengths are observed, Mo(1)−O(5) = 2.179(2) Å vs. Mo(1)−O(6) = 2.120(2) Å and Mo(2)−O(9) = 2.157(2) Å vs. Mo(2)−O(10) = 2.135(3) Å. Again, the differences are smaller than those observed in various compounds with an operating *trans* influence. For example, in $[\{Mo_2O_4(C_2O_4)_2(H_2O)_2\}_2\{[Ln(H_2O)_4]_2(C_2O_4)\}]\cdot 7H_2O$ ($Ln = La^{3+}$, Ce^{3+})[23] the bis(bidentate) oxalate ions link two Mo^V_2 entities and two rare earth cations with two distinctly different bond lengths, 2.244(7)−2.251(3) Å vs. 2.143(3)−2.159(7) Å. These observations imply that there are other factors that influence the molybdenum-to-oxalato bond lengths.

Crystal Structure of $(MeNC_5H_5)_6[\{Mo_2O_4(\eta^2\text{-}C_2O_4)_2\}_2(\mu_4\text{-}C_2O_4)]$ *(2)*

The crystal structure of **2** consists of tetranuclear $[\{Mo_2O_4(\eta^2\text{-}C_2O_4)_2\}_2(\mu_4\text{-}C_2O_4)]^{6-}$ anions (Figure 2) and *N*-methylpyridinium cations. The anion may be viewed as two $\{Mo_2O_4\}^{2+}$ subunits linked to each other through a μ_4-bridging oxalate ion. The Mo−Mo separation in the $\{Mo_2O_4\}^{2+}$ subunits, 2.5655(4) Å, is in agreement with the value expected for a single metal−metal bond. Each metal centre is attached to a bidentate oxalate ion, the corresponding molybdenum−oxygen distances are 2.0846(16) and 2.0920(18) Å. The terminal oxalate ions are tilted in an umbrella-like manner towards the other half of the anion, as if to shield the bridging oxalate ion. The relatively short distances, 2.7169(22) and 2.7359(23) Å, between a pair of coordinated oxygen atoms of the terminal oxalate ions to the oxygen atom of the μ_4-oxalate ion add support to this observation. This structural feature is readily apparent in Figure 2a. The four molybdenum atoms are related by an improper fourfold rotation axis, which passes through the C−C vector of the μ_4-oxalate ion and the centres of both $Mo(O_b)_2Mo$ rhombic units (Figure 2b). Consequently, the two metal−metal bond vectors are perpendicular to each other. Each oxygen atom of the bridging oxalate ion is coordinated to a different metal centre at a relatively long distance of 2.3678(16) Å. The lengthening of this bond when compared to the molybdenum-to-terminal-oxalate bond lengths may be explained in terms of the *trans* influence of

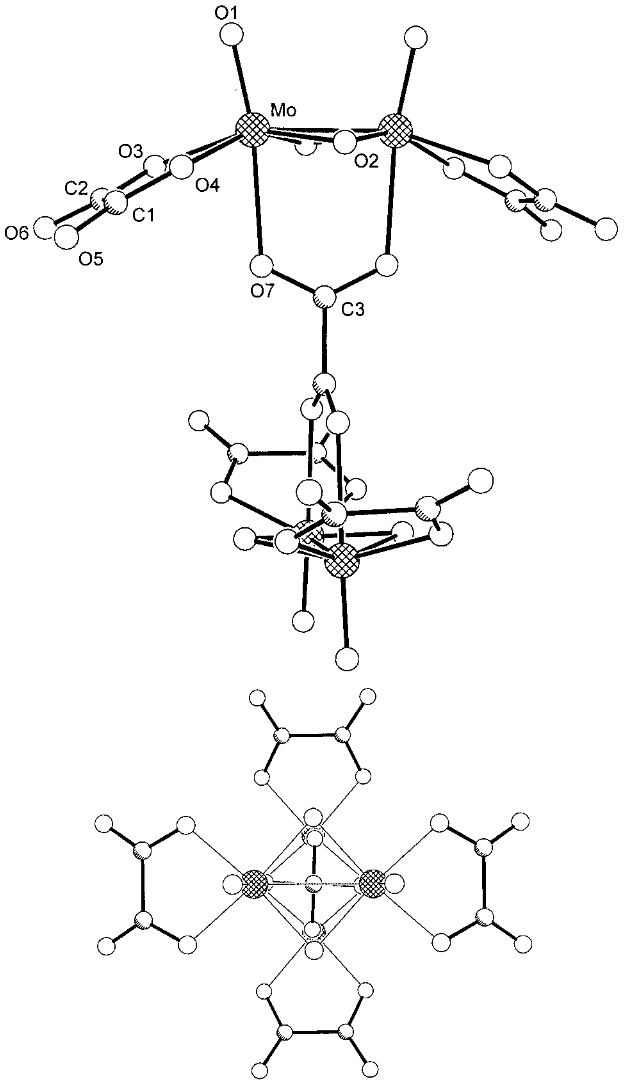

Figure 2. (a) (top) $[\{Mo_2O_4(\eta^2\text{-}C_2O_4)_2\}_2(\mu_4\text{-}C_2O_4)]^{6-}$, the anionic part of **2**, with the μ_4-oxalate ion in a staggered conformation; selected bond lengths [Å]: Mo−O(1) 1.678(2), Mo−O(2) 1.9397(18), Mo−O(2)[a] 1.9423(17), Mo−O(3) 2.0920(18), Mo−O(4) 2.0846(16), Mo−O(7) 2.3678(16), Mo−Mo[a] 2.5655(4), C(3)−O(7) 1.2548(19), C(3)−C(3)[b] 1.532(6); symmetry operations: [a] $-x, -y - 0.5, z$; [b] $-y - 0.25, x - 0.25, -z + 0.25$; (b) (bottom) the tetranuclear anion viewed along the improper fourfold axis

Table 3. Selected geometric parameters [Å] of $\{Mo_2O_4\}^{2+}$ units with a third bridging ligand L[a]

	Mo−Mo	L	Mo−L
2	2.5655(4)	oxalate	2.3678(16)
3	2.5786(4), 2.5770(4)	oxalate	2.355(2)−2.395(2)
$[Mo^{II}{}_2Mo^{V}{}_2O_4(OH)_4(\mu_4\text{-}CO_3)(CO)_2(PMe_3)_6]$[24]	2.5522(9)	carbonate	2.419(3)
$[(Mo_2O_4)_3(\mu_6\text{-}CO_3)(\mu_2\text{-}CO_3)_3(\mu_2\text{-}OH)_3]^{5-}$ [4] [b]	2.5884(6)	carbonate	2.355(3)
$\{Na[(Mo_2O_4)_3(\mu_6\text{-}SO_3)(\mu_2\text{-}SO_3)_3(\mu_2\text{-}O)_3]_2\}^{15-}$ [5] [c]	2.597(5)	sulfate(IV)	2.36(2)
$[Mo_2O_4(\mu_2\text{-}SO_3)(SO_3)_4]^{8-}$ [5]	2.5872(18)	sulfate(IV)	2.27(1)
$[\{Mo_2O_4(\eta^2\text{-}mal)_2\}_2(\mu_4\text{-}mal)]^{6-}$ [25] [d]	2.555	malonate	2.321

[a] A multidentate oxygen donor ligand L coordinates to the dinuclear unit in all cited examples through two of its oxygen atoms, and to each metal centre with one. With the exception $[Mo_2O_4(\mu_2\text{-}SO_3)(SO_3)_4]^{8-}$, it binds in this manner to two or three $\{Mo_2O_4\}^{2+}$ units. [b] A μ_6-carbonate unit links three dinuclear units. [c] A μ_6-sulfate(IV) unit links three dinuclear units. [d] mal = $CH_2(COO)_2{}^{2-}$. A μ_4-malonate unit links two dinuclear units.

the terminal oxo group. A comparison with other $\{Mo_2O_4\}^{2+}$ compounds where multidentate oxygen donor ligands also coordinate to a pair of molybdenum atoms through two oxygen donor atoms in *trans* positions to the terminal oxo groups shows that the distances in **2** are within the normal range (Table 3).

The bridging oxalate ion is in a completely staggered conformation. The C−O distances of the μ_4-oxalate ion are equal, at 1.2548(19) Å, suggesting a bond character between a single and a double bond. For comparison, two sets of C−O distances are displayed within the bidentate oxalate ions, short ones, 1.216(3) and 1.219(3) Å, typical of localized double bonds, and longer ones, 1.291(3) and 1.294(3) Å. Hexaanions with two dinuclear subunits linked through a tetradentate oxalate ion have been observed before. Thio derivatives of the dinuclear unit, $\{Mo_2O_2(\mu_2\text{-}O)(\mu_2\text{-}S)\}^{2+}$ and $\{Mo_2O_2(\mu_2\text{-}S)_2\}^{2+}$, assemble in almost the same fashion as shown by $[\{Mo_2O_3S(\eta^2\text{-}C_2O_4)_2\}_2(\mu_4\text{-}C_2O_4)]^{6-}$ and $[\{Mo_2O_2S_2(\eta^2\text{-}C_2O_4)_2\}_2(\mu_4\text{-}C_2O_4)]^{6-}$, respectively.[26−28] The same structural type also occurs among very rare oxotungsten(V) compounds, such as $[\{W_2O_2S_2(\eta^2\text{-}C_2O_4)_2\}_2(\mu_4\text{-}C_2O_4)]^{6-}$.[28] Another example, $[Mo_4O_4S_2X_2(C_2O_4)_5]^{6-}$ (X = O or S), consists of one $\{Mo_2O_2(\mu_2\text{-}S)_2\}^{2+}$ unit, while the other displays a disorder in the double bridge.[29] The bridging atoms are partially oxygen and partially sulfur atoms. In contrast to a completely staggered configuration of the oxalate ion in **2**, the μ_4-oxalate ions in all the cited examples are planar. Ab initio MO calculations on the $[\{Mo_2O_4(\eta^2\text{-}C_2O_4)_2\}_2(\mu_4\text{-}C_2O_4)]^{6-}$ anion revealed the isomer with the staggered conformation of the oxalate ion to be the energetically more favoured one (Figure 3). The difference between the calculated energy of the anion with a staggered oxalate ion and that with a planar oxalate ion is 18 kcal/mol. AM1 and ab initio calculations on the oxalate dianion itself also indicated a slight preference for a completely staggered D_{2d} structure over a planar D_{2h} structure.[30] Bearing in mind that the bond lengths between the molybdenum atom and the oxalate oxygen atom in **2** are relatively long, this agreement is not surprising. The calculated barrier to rotation about the C−C bond in the oxalate dianion is smaller than in our case, ca. 5 kcal/mol. An oxalate ion coordinated to different metal ions usually adopts a planar or near-planar form. Only a few deviations from planarity have been reported so far. In $[Ni(L1)(C_2O_4)]_n{\cdot}nH_2O$ (L1 represents a tetraaza macrocyclic ligand)[31] and $[Cu(C_2O_4)(H_2O)(4\text{-}apy)_2]_n$ (4-apy = 4-aminopyridine)[32] the twist angles of the 1,1′-bis(monodentate) oxalate ion are 103° and 28°, respectively. In both these compounds the nonbonded oxalate oxygen atoms participate in significant hydrogen bonding interactions suggesting that these have an important influence over the ligand's conformation. In a recent study of the anhydrous alkali oxalates, in combination with K^+, Rb^+ and Cs^+ cations, both planar and staggered oxalate conformations were observed, showing that the conformation is determined mainly by packing effects.[33] On the other hand, the electronic structure calculations for the model compounds $[(HCOO)_3M_2(\mu_4\text{-}C_2O_4)M_2(HCOO)_3]$ ($HCOO^-$ stands for formate; and M_2 stands for pairs of Mo^{II} or W^{II} atoms linked by quadruple metal−metal bonds) employing density functional theory predicted the structure with the planar oxalate ion to be energetically more favoured than the one with the completely staggered oxalate ion by ca. 8 kcal/mol. This latter result is in line with the concept that the electronic coupling of M_2 units is maximized when the oxalate ion is in a planar conformation.[34]

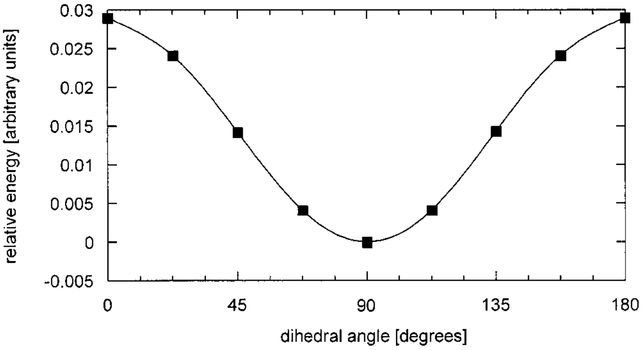

Figure 3. Relative energy of $[\{Mo_2O_4(\eta^2\text{-}C_2O_4)_2\}_2(\mu_4\text{-}C_2O_4)]^{6-}$ as a function of the dihedral angle in the μ_4-oxalate ion; 0.01 units correspond to 6.27 kcal/mol

Two other multidentate oxygen donor ligands, the malonate and sulfate ions, also form similar tetranuclear hexaanions in combination with the $Mo^{V}{}_2$ unit — $[\{Mo_2O_4(\eta^2\text{-}$

mal)$_2$}$_2$(μ_4-mal)]$^{6-}$,[25] and [{$Mo_2O_2S_2(\eta^2-SO_4)_2$}$_2$($\mu_4$-$SO_4$)]$^{6-}$.[35] The latter is the closest structural relative to the anion in **2**. The inherent improper fourfold rotation symmetry of the μ_4-SO_4^{2-} ligand leads to the perpendicular orientation of the two {$Mo_2O_2(\mu_2\text{-}S)_2$}$^{2+}$ subunits. The elongated Mo_4 tetrahedron has two short (approx. 2.8 Å) and four long (approx. 6.8 Å) Mo−Mo distances. The corresponding distances within the Mo_4 tetrahedron in **2** are 2.5655(4) Å and 7.5913(4) Å.[36]

The fold angle in **2**, 160.21(5)°, is larger than in other {Mo_2O_4}$^{2+}$ compounds (see Table 2). Keeping the metal−metal bond length within the normal range, the less folded bridging moiety, where the value of the fold angle is larger, induces changes in the angles within the $Mo_2(O_b)_2$ rhombus, especially in the O_b−Mo−O_b angles, which become larger. In some of the selected examples in Table 2, the {Mo_2O_4}$^{2+}$ units are fused together by sharing bridging oxygen atoms. It is pertinent to note that such an assembly also induces stress upon the internal dimensions of the constituent dinuclear blocks.

Crystal Structure of ($MeNC_5H_5$)$_2$[$Mo_8O_{16}(OMe)_8(\mu_8\text{-}C_2O_4)$] (3)

This compound consists of cyclic octanuclear [$Mo_8O_{16}(OMe)_8(\mu_8\text{-}C_2O_4)$]$^{2-}$ anions and *N*-methylpyridinium cations. As the centre of the ring lies on an inversion centre, the asymmetric unit consists of one half of the anion. Four {Mo_2O_4}$^{2+}$ blocks are connected by pairs of methoxide ligands, forming a ring around the oxalate anion (Figure 4a). The methoxide ions fold out from the ring, whereas the oxo groups fold into the ring. Short metal−metal distances [2.5770(4) Å and 2.5786(4) Å] within the dinuclear blocks alternate with longer non-bonding Mo···Mo contacts [3.2577(4) and 3.2655(4) Å] between the neighbouring dinuclear blocks. Each of the molybdenum centres displays a pseudo-octahedral coordination sphere consisting of six oxygen atoms. The terminal oxygen atoms lie at 1.683(2)−1.688(2) Å, bridging oxygen atoms at 1.926(2)−1.946(2) Å, and bridging methoxide ligands at 2.084(2)−2.122(2) Å. An oxygen atom of the central oxalate ion occupies the position *trans* to the molybdenyl group at a significantly longer distance, 2.355(2)−2.395(2) Å. It also functions as a third bridge between a pair of molybdenum atoms linked by methoxide ligands. The fold angles of the {Mo_2O_4}$^{2+}$ units are 156.43(14)° and 156.83(18)°. All metal atoms, terminal oxo groups and the oxalate ion lie in the plane. One half of the bridging methoxide ions and the bridging oxo groups lie above, and the other half below this plane (Figure 4b). The central oxalate ion is disordered over two positions. The C−O distances of the oxalate ion are in the 1.287(6)−1.317(7) Å range.

The planar configuration of the ring in **3** contrasts with the puckered arrangement observed in [$Mo_8O_{16}(OMe)_8(R\text{-}py)_4$], with a vacant central cavity.[37] However, the Mo−Mo bond lengths and the Mo···Mo non-bonding contacts in the two are basically the same. The pair illustrates how the oxalate or pyridine ligands influence the conformation of the ring obtained upon the assembly of four {Mo_2O_4}$^{2+}$ building blocks.

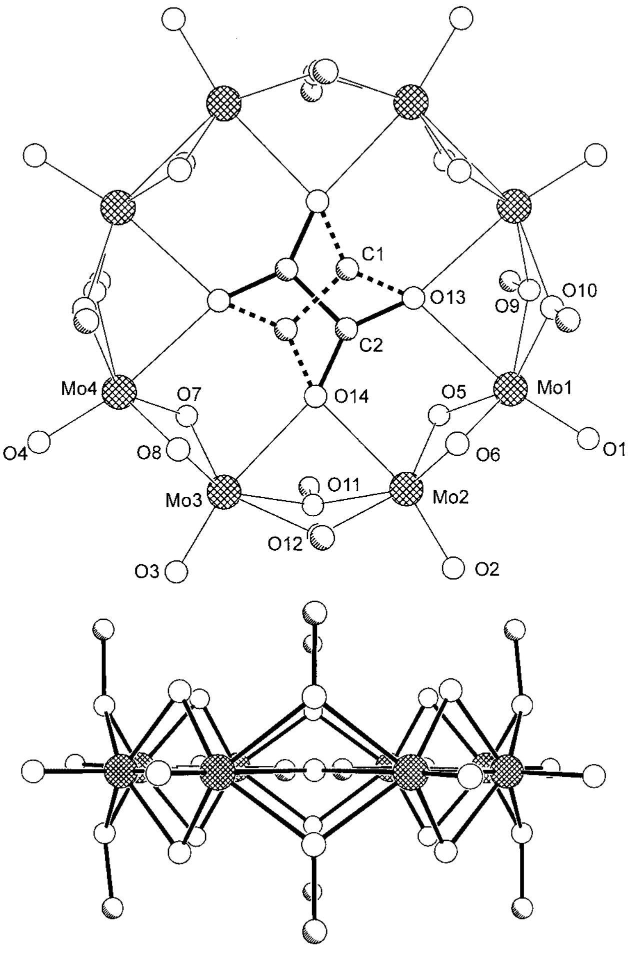

Figure 4. (a) (top) [$Mo_8O_{16}(OMe)_8(\mu_8\text{-}C_2O_4)$]$^{2-}$, the anionic part in **3**, with the oxalate ion disordered over two positions; selected bond lengths [Å]: Mo(1)−Mo(2) 2.5786(4), Mo(3)−Mo(4) 2.5770(4), Mo(1)−O(13) 2.386(2), Mo(2)−O(14) 2.355(2), Mo(3)−O(14) 2.373(2), Mo(4)−O(13)[a] 2.395(2); symmetry operation: [a] $2 - x$, $1 - y$, $2 - z$; (b) (bottom) side view of the octanuclear anion showing the planar conformation of the ring

The anion [$Mo_8O_{16}(OMe)_8(\mu_8\text{-}C_2O_4)$]$^{2-}$ has been obtained before by the reaction of α-[$(n\text{-}C_4H_9)_4N$]$_4$[Mo_8O_{26}] with rhodizonic acid.[38] Its formation was explained in terms of a carbonyl insertion reaction coupled with ligand dissociation and redox processes. The same authors also reported the crystal structure of an ethoxide-bridged derivative, [$Mo_8O_{16}(OEt)_8(\mu_8\text{-}C_2O_4)$]$^{2-}$.[39] The same structural motif — four dinuclear building blocks forming a cycle — is also produced upon the linkage of {$Mo_2O_2(\mu_2\text{-}S)_2$}$^{2+}$ units through pairs of hydroxide bridges. The neutral cycle with the [$Mo_8S_8O_8(OH)_8$] composition can encapsulate various ligands, such as oxalate,[28,40a] molybdate(VI)[40b] or tungstate(VI) ions.[40c] The {$Mo_2O_2(\mu_2\text{-}S)_2$}$^{2+}$ unit forms in the presence of hydroxide ions even larger neutral cycles, which incorporate oxygen-donor guests with direct covalent interactions between the oxygen and molybdenum atoms. The inorganic backbone adapts its size and geometry to that of the guest anion. In the case of glutarate, a decanuclear ring was obtained, while with larger anions such as pimelate and trimesate, dodecanuclear rings were formed.[40]

Crystal Structure of $[MeNC_5H_2(Me)_3]_2[HNC_5H_2(Me)_3]_2[Mo_2O_3(\eta^2\text{-}C_2O_4)_4]$ *(4)*

The dinuclear complex $[Mo_2O_3(\eta^2\text{-}C_2O_4)_4]^{4-}$ (**4**; Figure 5) displays a centrosymmetric structure consisting of an *anti*-$\{Mo_2O_2(\mu_2\text{-}O)\}^{4+}$ core (Scheme 2). *N*-methylated collidine and protonated collidine molecules serve as countercations. Two molybdenum atoms are connected by a single oxygen atom, O(2), lying on the inversion centre. Consequently, the Mo−O−Mo bridge is linear with symmetrical Mo−O(2) bond lengths of 1.8534(2) Å. The two terminal oxygen atoms are *trans* to each other. Insofar as the dimensions of the *anti*-$\{Mo_2O_2(\mu_2\text{-}O)\}^{4+}$ unit are concerned, these are similar to other compounds containing this fragment.[41] Two bidentate oxalate ligands complete a distorted octahedral environment of each metal atom. The coordinated oxygen atoms of one oxalate ion, with bond lengths to the molybdenum atom of 2.032(2) and 2.081(2) Å, are *cis* to the Mo=O group. The corresponding bite angle is 78.37(9)°. The other oxalate ion binds with two distinctly different bond lengths, 2.0869(19) and 2.217(2) Å. The longer one is, as expected, *trans* to the terminal oxo group. The oxalate bite angle is smaller, 73.87(7)°. The oxalate bite angles are largely determined by the metal−oxygen distances: when these are longer than 2.1 Å, the oxygen−metal−oxygen angles become smaller than 80°.[42]

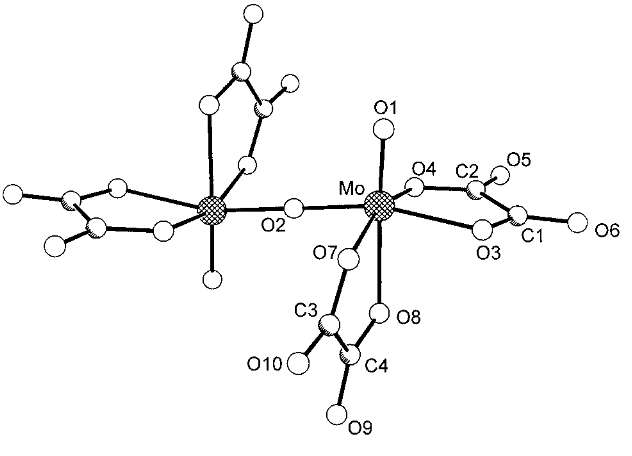

Figure 5. $[Mo_2O_3(\eta^2\text{-}C_2O_4)_4]^{4-}$ ion in **4**; selected bond lengths [Å]: Mo−O(1) 1.668(3), Mo−O(2) 1.8534(2), Mo−O(3) 2.081(2), Mo−O(4) 2.032(2), Mo−O(7) 2.0869(19), Mo−O(8) 2.217(2)

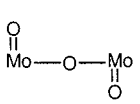

$$\overset{O}{\overset{\|}{Mo}}-O-\underset{O}{\underset{\|}{Mo}}$$

Scheme 2. *anti*-$\{Mo_2O_3\}^{4+}$ structural unit

Vibrational Spectroscopy

Although the oxalate absorption bands in the infrared spectra reflect its binding modes,[43] the overlap of some with pyridine absorptions prevents straightforward assignations. Among three sets of the characteristic oxalate bands, $\nu_{as}(OCO)$, $\nu_s(OCO)$ and $\delta(OCO)$, the carbon−oxygen asymmetric and symmetric stretching frequencies show the highest sensitivity to the metal coordination and thus to the binding mode employed. In addition, the metal−oxygen bond lengths also affect the number of bands.[44] The influence of the asymmetric binding on the infrared bands is clearly observed in the infrared spectra of $(MeNC_5H_5)_{2n}[Mo_2O_4(C_2O_4)Cl_2]_n$ and $(3\text{-}MePyH)_{2n}[Mo_2O_4(C_2O_4)Cl_2]_n$ where the bis(bidentate) oxalate ion bridges two metal centres in a highly asymmetric fashion, 2.172(2) vs. 2.312(2) and 2.1684(15) vs. 2.3183(16) Å, respectively.[13] Two sets of $\nu_{as}(OCO)$ [at 1671 and 1633 cm^{-1} for the $MeNC_5H_5^+$ compound, and at 1671 and 1633 cm^{-1} for the 3-MePyH$^+$ compound] and $\nu_s(OCO)$ bands [at 1354, 1306 and 1288 cm^{-1} for the $MeNC_5H_5^+$ compound, and at 1353, 1302 and 1264 cm^{-1} for the 3-MePyH$^+$ compound] are observed.

In **3**, with one type of oxalate ligand, each of the oxalate oxygen atoms bridges two molybdenum atoms with metal−oxygen distances of approximately the same length. The bands at 1659, 1635 [$\nu_{as}(OCO)$], 1336, 1290 [$\nu_s(OCO)$] and 813 cm^{-1} [$\delta(OCO)$] are in accordance with expectations.[43] The terminal, bidentate binding mode in **1** gives rise to bands at 1705, 1667, 1633 [$\nu_{as}(OCO)$], 1372, 1287 [$\nu_s(OCO)$] and at 780 cm^{-1} [$\delta(OCO)$]. Their frequencies agree very well with those reported for $Ba[Mo_2O_4(C_2O_4)_2(H_2O)_2]\cdot 3H_2O$ {1710, 1680, 1653 [$\nu_{as}(OCO)$]; 1430, 1289 [$\nu_s(OCO)$]; 793 cm^{-1} [$\delta(OCO)$]}[19] and other compounds containing a bidentate oxalate ion.[45] The occurrence of a bidentate oxalate ion is also evident in the spectrum of **4** where the bands occur at 1709, 1682, 1633 [$\nu_{as}(OCO)$], 1337, 1259 ν_s[(OCO)] and 799 cm^{-1} [$\delta(OCO)$]. A multitude of bands {1705, 1681, 1657, 1633, 1574 [$\nu_{as}(OCO)$]; 1360, 1322, 1288 [$\nu_s(OCO)$]; 828, 800 cm^{-1} [$\delta(OCO)$]} in the spectrum of **2** indicates both the bidentate and tetradentate binding modes of the oxalate ion. These are similar to those observed in $[H_3N(CH_2)_3NH_3]_3[Mo_4S_4O_4(C_2O_4)_5]\cdot 4.5H_2O$ [bands at 1716, 1688, 1600, 1506 in the $\nu_{as}(OCO)$ region; 1391, 1321, 1242 in the $\nu_s(OCO)$ region and 830, 794 cm^{-1} in the $\delta(OCO)$ region].[28]

Bands in the 1000−900 cm^{-1} region are associated with the Mo=O stretching vibrations. These are seen as strong bands at 949, 939 and 927 cm^{-1} for **1**, 958, 942 and 903 cm^{-1} for **2**, and for **3** and **4** as a single band at 962 and 960 cm^{-1}, respectively.

General Considerations

As observed before,[13−15,46] methanol and pyridines provide a medium where the formation of the $\{Mo_2O_4\}^{2+}$ fragment from the mononuclear halooxomolybdate(v) is a fast and reproducible process. The dinuclear unit with three coordination sites per metal atom and the oxalate ion is a system where the variation of the amount of one with respect to the other can produce discrete clusters when the amounts of the oxalate ion are large, or a polymeric material when the amounts of the oxalate ion are small. In the former case, $[Mo_2O_4(\eta^2\text{-}C_2O_4)_2py_2]^{2-}$ (**1**) and $[\{Mo_2O_4(\eta^2\text{-}C_2O_4)_2\}_2(\mu_4\text{-}C_2O_4)]^{6-}$ (**2**) were obtained. In **1** the oxalate ion occupies two out of three coordination sites of each metal atom in a bidentate fashion. One of the coordinated oxalate oxygen atoms is *cis* to the Mo=O group, and the other is in a less favourable *trans* position. Pyridine ligates to the remaining, third site. Considering both metal centres, two distinct geometries are possible. In **1**, the two pyridine ligands are on the opposite sides of the plane defined by a pair of Mo=O groups (*trans* to each other). The two pyridine ligands can also lie on the same side of the plane (*cis* to each other). The reaction conditions employed in the preparation of **1** apparently favour the *trans* isomer. Employing a huge excess of the oxalate ion afforded $[\{Mo_2O_4(\eta^2\text{-}C_2O_4)_2\}_2(\mu_4\text{-}C_2O_4)]^{6-}$ (**2**), where all three coordination sites of each metal centre are occupied with oxygen-donor ligands. Two belong to the bidentate oxalate ion and the third one to the bridging oxalate ion. Although the reaction medium for the preparation of **2** is mostly pyridine, pyridine does not coordinate. Reducing the ratio of oxalate vs. molybdate produces either a polymeric $[Mo_2O_4(C_2O_4)Cl_2]_n^{2n-}$, with one oxalate ion per dinuclear unit,[13] or a discrete octanuclear $[Mo_8O_{16}(OMe)_8(\mu_8\text{-}C_2O_4)]^{2-}$ (**3**) with one oxalate ion for every four dinuclear units, the major difference between the two synthetic procedures being the presence of pyridine. While the polymeric species is obtained in pyridine, the reaction mixture used in the case of **3** does not contain any. Methanol not only provides the reaction medium in the preparation of **3**, it is also a source of methoxide ions, which coordinate to the molybdenum atom and serve as bridges in the linkage of $\{Mo_2O_4\}^{2+}$ units. The role that methanol plays in the reaction mixtures merits additional comment as it is also consumed in the in situ formation of *N*-methylpyridinium cations. Their formation at elevated temperature requires apart from methanol, also pyridine and oxalic acid. *N*-Alkylation takes place when other pyridines are used as substrates as well, for example 2,4,6-collidine in the formation of **4**. The exact nature of this process is currently under investigation.[47] When no methanol is used, the only product isolated so far was $(PyH)_2[Mo_2O_4(\eta^2\text{-}C_2O_4)_2py_2]$, provided that a sufficient amount of the oxalate ion was present.

It is pertinent to mention briefly a series of structurally related species, dinuclear *cis*-$[Mo_2O_2(\mu_2\text{-}S)_2(\eta^2\text{-}C_2O_4)_2(H_2O)_2]^{2-}$, tetranuclear $[\{Mo_2O_2(\mu_2\text{-}S)_2(\eta^2\text{-}C_2O_4)_2\}_2(\mu_4\text{-}C_2O_4)]^{6-}$ and octanuclear $[Mo_8O_8S_8(OH)_8(\mu_8\text{-}C_2O_4)]^{2-}$, which are formed in the reactions between the thio-bridged dimer $\{Mo_2O_2(\mu_2\text{-}S)_2\}^{2+}$ and oxalate ions in aqueous media.[28,40e,40f] It was observed that the reaction products depend more upon the pH of the reaction medium than the stoichiometry. At pH ≈ 1.5, the dinuclear species is obtained, in less acidic medium, at pH ≈ 4, the tetranuclear one and at pH > 5, the octanuclear one. The binding modes of the oxalate ion were described as the competition between the chelating and the templating role of the ligand. The analogy between the thio-bridged species and the anions of **1**, **2** and **3** is unfortunately limited to their structures only. The same pattern of assembly of basic dinuclear units to form larger oligonuclear species can be recognized within the two series.

The preparation of **4** opens new perspectives. Similar amounts of the reagents were used as for the preparations of **1** or **2** with 2,4,6-collidine instead of pyridine. Given the low coordinating ability of 2,4,6-collidine due to methyl substituents in the *ortho* positions, the oxalate ion, as the only other ligand present in the reaction mixture, was forced to occupy more than two coordination sites in each metal atom environment. A singly oxo-bridged dimer, $\{Mo_2O_3\}^{4+}$, was formed. The four coordination sites of each metal atom are occupied by a pair of bidentate oxalate ions. It remains open for further studies to investigate how this system would respond to a reduced amount of oxalate ions, whether the oxalate ion would adopt the bis(bidentate) binding mode and as such connect dinuclear units, $\{Mo_2O_3\}^{4+}$ fragments in this case, into polymeric structures. It also seems feasible that the use of non-coordinating solvents could enable the coordination of the oxalate ion in less common binding modes and thus the synthesis of more complex architectures.

Conclusion

A series of discrete oxalato complexes of molybdenum(V) was accessed by solvothermal reactions of mononuclear halooxomolybdates(V) with oxalic acid. The oxalate ion binds to the dinuclear units, $\{Mo_2O_4\}^{2+}$ or $\{Mo_2O_3\}^{4+}$, as a terminal bidentate ligand as observed in $[Mo_2O_4(\eta^2\text{-}C_2O_4)_2py_2]^{2-}$ (**1**) and $[Mo_2O_3(\eta^2\text{-}C_2O_4)_4]^{4-}$ (**4**) or bridges two or four $\{Mo_2O_4\}^{2+}$ units as observed in $[\{Mo_2O_4(\eta^2\text{-}C_2O_4)_2\}_2(\mu_4\text{-}C_2O_4)]^{6-}$ (**2**) and $[Mo_8O_{16}(OMe)_8(\mu_8\text{-}C_2O_4)]^{2-}$ (**3**), respectively.

Experimental Section

General Remarks: Reactions were carried out in sealed glass tubes under autogenous pressure. Reagents were purchased from Aldrich and used without further purification. $(PyH)_2[MoOCl_5]$ and $(PyH)[MoOBr_4]$ were prepared by minor modification of a published procedure.[48] The IR and far-IR spectra were measured on solid samples as Nujol or poly(chlorotrifluoroethylene) mulls using a Perkin−Elmer 2000 series FT-IR spectrometer. Elemental analyses were performed by the Chemistry Department service at the University of Ljubljana.

$(MeNC_5H_5)_2[Mo_2O_4(\eta^2\text{-}C_2O_4)_2py_2]$ (1): A mixture of $(PyH)_2[MoOCl_5]$ (100 mg, 0.223 mmol), $H_2C_2O_4\cdot 2H_2O$ (100 mg, 0.793 mmol), pyridine (4 mL), methanol (0.5 mL) and acetonitrile (0.5 mL) was placed in a glass tube which was sealed and subsequently heated in an electric oven maintained at 115 °C for 120 h. After cooling to room temperature, orange crystals of compound **1** were isolated in 40% yield (35 mg). IR: $\tilde{\nu}$ = 3047 (w), 2915 (w), 2851 (w), 1705 (vs), 1667 (vs), 1633 (vs), 1603 (vs), 1584 (s), 1494 (s), 1450 (s), 1372 (s), 1287 (m), 1254 (m), 1241 (m), 1216 (m), 1192 (m), 1163 (m), 1073 (m), 1015 (m), 949 (s), 939 (s), 927 (s), 897 (s), 780 (vs), 758 (vs), 734 (vs), 685 (vs), 649 (m), 639 (m), 524 (m), 482 (s), 451 (w), 435 (w), 348 (w), 320 (vs), 257 (s) cm^{-1}.

$C_{26}H_{26}Mo_2N_4O_{12}$ (778.39): calcd. C 40.12, H 3.37, N 7.20; found C 40.25, H 3.48, N 7.08.

$(MeNC_5H_5)_6[\{Mo_2O_4(\eta^2\text{-}C_2O_4)_2\}_2(\mu_4\text{-}C_2O_4)]$ (2): A mixture of $(PyH)_2[MoOCl_5]$ (50 mg, 0.111 mmol), $H_2C_2O_4{\cdot}2H_2O$ (150 mg, 1.19 mmol), pyridine (4 mL), methanol (0.5 mL) and acetonitrile (0.5 mL) was placed in a glass tube which was sealed and subsequently heated for in an electric oven maintained at 115 °C 120 h. After cooling to room temperature, the reaction mixture consisted of a dark solution and a black oil. Orange-red crystals formed after a period of two weeks. Yield 43% (18 mg). IR: $\tilde{\nu}$ = 3390 (m), 3136 (w), 3040 (m), 1705 (vs), 1681 (vs), 1657 (vs), 1633 (vs), 1574 (vs), 1494 (vs), 1449 (w), 1360 (vs), 1322 (vs), 1288 (vs), 1229 (vs), 1188 (vs), 1059 (w), 1026 (w), 958 (vs), 942 (vs), 903 (s), 879 (m), 828 (m), 800 (vs), 770 (vs), 737 (vs), 682 (vs), 649 (m), 528 (vs), 467 (m), 449 (m), 411 (w), 395 (w), 359 (m), 326 (w), 311 (vs), 235 (w) cm^{-1}. $C_{46}H_{48}Mo_4N_6O_{28}$ (1516.7): calcd. C 36.43, H 3.19, N 5.54; found C 36.25, H 3.28, N 5.41.

$(MeNC_5H_5)_2[Mo_8O_{16}(OMe)_8(\mu_8\text{-}C_2O_4)]$ (3): A mixture of $(PyH)_2[MoOCl_5]$ (100 mg, 0.223 mmol), $H_2C_2O_4{\cdot}2H_2O$ (22 mg, 0.175 mmol), methanol (4.5 mL) and acetonitrile (0.5 mL) was placed in a glass tube which was sealed and subsequently heated in an electric oven maintained at 115 °C for 120 h. After cooling to room temperature, large orange crystals of compound **3** were separated manually from the orange microcrystalline phase. The yield based on **3** was 14% (6 mg). IR: $\tilde{\nu}$ = 3143 (w), 3092 (w), 1659 (vs), 1635 (vs), 1585 (m), 1492 (m), 1336 (m), 1290 (m), 1224 (w), 1190 (m), 1162 (w), 1015 (vs), 962 (vs), 813 (vs), 755 (vs), 724 (s), 680 (s), 528 (vs), 466 (vs), 437 (m), 412 (m), 380 (s), 288 (w), 275 (s), 217 (m), 151 (w) cm^{-1}. $C_{22}H_{40}Mo_8N_2O_{28}$ (1548.1): calcd. C 17.07, H 2.60, N 1.81; found C 16.95, H 2.51, N 1.92.

$[MeNC_5H_2(Me)_3]_2[HNC_5H_2(Me)_3]_2[Mo_2O_3(\eta^2\text{-}C_2O_4)_4]$ (4): A mixture of $(PyH)[MoOBr_4]$ (120 mg, 0.235 mmol), $H_2C_2O_4{\cdot}2H_2O$ (100 mg, 0.793 mmol), 2,4,6-collidine (4 mL), methanol (0.5 mL) and acetonitrile (0.5 mL) was placed in a glass tube which was sealed and subsequently heated in an electric oven maintained at 115 °C for 120 h. After cooling to room temperature, large black crystals of compound **4** were isolated in 47% yield (61 mg). IR: $\tilde{\nu}$ = 2920 (vs), 2849 (vs), 2671 (m), 2580 (m), 1912 (w), 1709 (vs), 1682 (vs), 1633 (vs), 1337 (m), 1274 (w), 1259 (m), 1224 (w), 1199 (m), 1171 (w), 1152 (w), 1039 (m), 997 (w), 960 (vs), 892 (m), 863 (w), 799 (vs), 786 (m), 721 (w), 535 (s), 517 (s), 477 (m), 445 (m), 366 (m), 350 (m), 312 (s), 264 (m), 220 (m), 193 (m). $C_{42}H_{52}Mo_2N_4O_{19}$ (1108.76): calcd. C 45.50, H 4.73, N 5.05; found C 45.68, H 4.59, N 4.97.

X-ray Crystallographic Study: The crystals were mounted on the tip of a glass fibre with a small amount of silicon grease and transferred to a goniometer head. Data were collected with a Nonius Kappa CCD diffractometer. For all compounds, data reduction and integration were performed with the software package DENZO-SMN.[49] Averaging of the symmetry-equivalent reflections largely compensated for the absorption effects. The coordinates of some or all of the non-hydrogen atoms were found by direct methods using the structure solution program SHELXS.[50] The positions of the remaining non-hydrogen atoms were located by use of a combination of least-squares refinement and difference Fourier maps with the SHELXL-97[50] program. Non-hydrogen atoms were refined with anisotropic displacement parameters. The hydrogen atoms were included in the structure factor calculations at idealized positions. The oxalate ion in **3** is disordered over two positions. The carbon atoms C(1) and C(2) of the disordered oxalate ion were refined anisotropically with the occupancy factors 0.51(1) and 0.49(1), respectively. Cell parameters and refinement results for compounds **1**−**4** are summarized in Table 4. CCDC-211525 (**1**), -211526 (**2**), -211527 (**3**) and -211528 (**4**) contain the supplementary crystallographic data for this paper. These data can be obtained free of charge at www.ccdc.cam.ac.uk/conts/retrieving.html [or from the Cambridge Crystallographic Data Centre, 12 Union Road, Cambridge CB2 1EZ, UK; Fax: (internat.) + 44-1223/336-033; E-mail: deposit@ccdc.cam.ac.uk].

Computational Details: Ab initio MO calculations on the $[\{Mo_2O_4(\eta^2\text{-}C_2O_4)_2\}_2(\mu_4\text{-}C_2O_4)]^{6-}$ ion at the HF/3-21G* level were performed in order to determine its energy as a function of the dihedral angle in the μ_4-oxalate ion. The Gaussian 98 suite of programs was used.[51] No geometry optimization was applied. The

Table 4. Crystallographic data for compounds **1**−**4**

	1	2	3	4
Empirical formula	$C_{26}H_{26}Mo_2N_4O_{12}$	$C_{46}H_{48}Mo_4N_6O_{28}$	$C_{22}H_{40}Mo_8N_2O_{28}$	$C_{42}H_{52}Mo_2N_4O_{19}$
Formula mass	778.39	1516.66	1548.08	1108.76
Crystal system	triclinic	tetragonal	triclinic	triclinic
Space group	$P\bar{1}$	$I4_1/acd$	$P\bar{1}$	$P\bar{1}$
T [K]	150(2)	200(2)	150(2)	293
a [Å]	9.7696(2)	16.5235(2)	7.4875(2)	9.2687(2)
b [Å]	11.5733(2)	16.5235(2)	10.9441(2)	11.3919(2)
c [Å]	14.0069(4)	40.6033(5)	14.3626(4)	12.3534(3)
α [°]	75.4096(10)	90	105.1707(10)	78.2266(8)
β [°]	86.8787(9)	90	103.5065(10)	69.0781(8)
γ [°]	69.0585(13)	90	105.5552(10)	86.8045(9)
V [Å^3]	1430.29(6)	11085.8(2)	1034.27(4)	1192.53(4)
Z	2	8	1	1
λ [Å]	0.71073	0.71073	0.71073	0.71073
μ [mm^{-1}]	0.949	0.980	2.439	0.605
Collected reflections	7850	10297	8539	7994
Unique reflections, R_{int}	4901, 0.0174	3164, 0.0206	4709, 0.0226	4159, 0.0129
Observed reflections	4405	2791	4092	3806
$R1$ [$I > 2\sigma(I)$]	0.0319	0.0299	0.0262	0.0334
$wR2$ [all data]	0.0822	0.0695	0.0605	0.1013

atomic coordinates were taken as obtained from the X-ray diffraction study.

Acknowledgments

We are grateful to the Slovenian Ministry of Education, Science and Sport for supporting this work through research grant PS-0508-0103. We also thank the same agency for funds to purchase the Nonius Kappa CCD diffractometer.

---

[1] [1a] *Polyoxometalates: From Platonic Solids to Anti-Retroviral Activity* (Eds.: M. T. Pope, A. Müller), Kluwer Academic Publishers, Dordrecht, **1994**. [1b] C. L. Hill (Guest editor), *Chem. Rev.* **1998**, *98*, 1−390.

[2] H. K. Chae, W. G. Klemperer, T. A. Marquart, *Coord. Chem. Rev.* **1993**, *128*, 209−224.

[3] C. Livage, E. Dumas, C. Marchal-Roch, G. Herve, *C. R. Acad. Sci. Paris, Ser. IIc* **2000**, *3*, 95−100.

[4] M. J. Manos, A. D. Keramidas, J. D. Woollins, A. M. Z. Slawin, T. A. Kabanos, *J. Chem. Soc., Dalton Trans.* **2001**, 3419−3420.

[5] M. J. Manos, J. D. Woollins, A. M. Z. Slawin, T. A. Kabanos, *Angew. Chem. Int. Ed.* **2002**, *41*, 2801−2805.

[6] [6a] R. C. Haushalter, F. W. Lai, *Inorg. Chem.* **1989**, *28*, 2904−2905. [6b] R. C. Haushalter, F. W. Lai, *Angew. Chem. Int. Ed. Engl.* **1989**, *28*, 743−746.

[7] C. du Peloux, P. Mialane, A. Dolbecq, J. Marrot, E. Riviere, F. Secheresse, *J. Mater. Chem.* **2001**, *11*, 3392−3396.

[8] E. Dumas, C. Sassoye, K. D. Smith, S. C. Sevov, *Inorg. Chem.* **2002**, *41*, 4029−4032.

[9] [9a] A. Müller, S. Dillinger, E. Krickemeyer, H. Bögge, W. Plass, A. Stammler, R. C. Haushalter, *Z. Naturforsch., Teil B* **1997**, *52*, 1301−1306. [9b] M. I. Khan, A. Müller, S. Dillinger, H. Bögge, Q. Chen, J. Zubieta, *Angew. Chem. Int. Ed. Engl.* **1993**, *32*, 1780−1782. [9c] M. I. Khan, Q. Chen, J. Salta, C. J. O'Connor, J. Zubieta, *Inorg. Chem.* **1996**, *35*, 1880−1901. [9d] A. Müller, C. Beugholt, P. Kögerler, H. Bögge, S. Bud'ko, M. Luban, *Inorg. Chem.* **2000**, *39*, 5176−5177. [9e] P. Mialane, A. Dolbecq, L. Lisnard, A. Mallard, J. Marrot, F. Secheresse, *Angew. Chem. Int. Ed.* **2002**, *41*, 2398−2401.

[10] C. du Peloux, P. Mialane, A. Dolbecq, J. Marrot, F. Secheresse, *Angew. Chem. Int. Ed.* **2002**, *41*, 2808−2810.

[11] L. A. Mundi, R. C. Haushalter, *Inorg. Chem.* **1990**, *29*, 2879−2881.

[12] M.-Y. Lee, S.-L. Wang, *Chem. Mater.* **1999**, *11*, 3588−3594.

[13] B. Modec, J. V. Brenčič, D. Dolenc, J. Zubieta, *J. Chem. Soc., Dalton Trans.* **2002**, 4582−4586.

[14] B. Modec, J. V. Brenčič, *J. Cluster Sci.* **2002**, *13*, 279−302.

[15] B. Modec, J. V. Brenčič, J. Zubieta, *J. Chem. Soc., Dalton Trans.* **2002**, 1500−1507.

[16] M. Cindrič, G. Pavlovič, V. Vrdoljak, B. Kamenar, *Polyhedron* **2000**, *19*, 1471−1478.

[17] F. H. Allen, O. Kennard, R. Taylor, *Acc. Chem. Res.* **1983**, *16*, 146−153.

[18] P. C. H. Mitchell, *J. Inorg. Nucl. Chem.* **1964**, *26*, 1967−1976 and references cited therein.

[19] F. A. Cotton, S. M. Morehouse, *Inorg. Chem.* **1965**, *4*, 1377−1381.

[20] P. C. H. Mitchell, *J. Chem. Soc. A* **1969**, 146−152.

[21] W. S. McDonald, *Acta Crystallogr., Sect. B* **1978**, *34*, 2850−2853.

[22] [22a] B. Kamenar, B. Kaitner, N. Strukan, *Croat. Chem. Acta* **1991**, *64*, 329−341. [22b] N. Strukan, M. Cindrič, B. Kamenar, *Acta Crystallogr., Sect. C* **2000**, *56*, 639−641.

[23] P. Mialane, A. Dolbecq, G. Costaz, L. Lisnard, J. Marrot, F. Secheresse, *Inorg. Chem. Commun.* **2002**, *5*, 702−705.

[24] [24a] E. Carmona, F. Gonzales, M. L. Poveda, J. M. Marin, J. L. Atwood, R. D. Rogers, *J. Am. Chem. Soc.* **1983**, *105*, 3365−3366. [24b] R. Alvarez, J. L. Atwood, E. Carmona, P. J. Perez, M. L. Poveda, R. D. Rogers, *Inorg. Chem.* **1991**, *30*, 1493−1499.

[25] T. Shibahara, H. Kuroya, K. Matsumoto, S. Ooi, *Inorg. Chim. Acta* **1981**, *54*, L75−L76.

[26] T. Shibahara, S. Ooi, H. Kuroya, *Bull. Chem. Soc. Jpn.* **1982**, *55*, 3742−3746.

[27] K. Mannemann, R. Mattes, *J. Chem. Res.* **1979**, *100*, 1343.

[28] A. Dolbecq, B. Salignac, E. Cadot, F. Secheresse, *Bull. Pol. Acad. Sci.* **1998**, *46*, 237−271.

[29] B. Kamenar, B. Kaitner, N. Strukan, *Vestn. Slov. Kem. Drus.* **1992**, *39*, 357−366.

[30] M. J. S. Dewar, Y. J. Zhang, *THEOCHEM* **1990**, *68*, 157−162.

[31] J. Chang Kim, J. Cho, A. J. Lough, *Inorg. Chim. Acta* **2001**, *317*, 252−258.

[32] O. Castillo, A. Luque, J. Sertucha, P. Roman, F. Lloret, *Inorg. Chem.* **2000**, *39*, 6142−6144.

[33] R. E. Dinnebier, S. Vensky, M. Panthöfer, M. Jensen, *Inorg. Chem.* **2003**, *42*, 1499−1507.

[34] B. E. Bursten, M. H. Chisholm, R. J. H. Clark, S. Firth, C. M. Hadad, A. M. MacIntosh, P. J. Wilson, P. W. Woodward, J. M. Zaleski, *J. Am. Chem. Soc.* **2002**, *124*, 3050−3063.

[35] C. G. Kim, D. Coucouvanis, *Inorg. Chem.* **1993**, *32*, 2232−2233.

[36] The distance 7.5913(4) Å is longer than the shortest Mo···Mo contact (approx. 6.5 Å) between adjacent anions.

[37] B. Modec, J. V. Brenčič, L. Golič, *Polyhedron* **2000**, *19*, 1219−1225.

[38] Q. Chen, S. Liu, J. Zubieta, *Angew. Chem. Int. Ed. Engl.* **1988**, *27*, 1724−1725.

[39] Q. Chen, S. Liu, J. Zubieta, *Inorg. Chem.* **1989**, *28*, 4433−4434.

[40] [40a] B. Salignac, S. Riedel, A. Dolbecq, F. Secheresse, E. Cadot, *J. Am. Chem. Soc.* **2000**, *122*, 10381−10389. [40b] A. Dolbecq, E. Cadot, F. Secheresse, *Chem. Commun.* **1998**, 2293−2294. [40c] A. Dolbecq, C. du Peloux, A.-L. Auberty, S. A. Mason, P. Barboux, J. Marrot, E. Cadot, F. Secheresse, *Chem. Eur. J.* **2002**, *8*, 349−356. [40d] A. Dolbecq, E. Cadot, F. Secheresse, *C. R. Acad. Sci. Paris, Ser. IIc* **2000**, *3*, 193−197. [40e] F. Secheresse, E. Cadot, A. Dolbecq, *J. Solid State Chem.* **2000**, *152*, 78−86. [40f] E. Cadot, F. Secheresse, *Chem. Commun.* **2002**, 2189−2197.

[41] [41a] R. L. Thompson, S. Lee, S. J. Geib, N. J. Cooper, *Inorg. Chem.* **1993**, *32*, 6067−6075. [41b] J. E. Drake, A. G. Mislankar, R. Ratnani, *Inorg. Chem.* **1996**, *35*, 2665−2673. [41c] L. Stelzig, S. Kötte, B. Krebs, *J. Chem. Soc., Dalton Trans.* **1998**, 2921−2926. [41d] C. J. Doonan, D. A. Slizys, C. G. Young, *J. Am. Chem. Soc.* **1999**, *121*, 6430−6436.

[42] N. F. Curtis, I. Ross, N. McCormick, T. N. Waters, *J. Chem. Soc., Dalton Trans.* **1973**, 1537−1548.

[43] N. F. Curtis, *J. Chem. Soc. A* **1968**, 1584−1587.

[44] I. Castro, J. Faus, M. Julve, A. Gleizes, *J. Chem. Soc., Dalton Trans.* **1991**, 1937−1944.

[45] P. Roman, A. Luque, C. Guzman-Miralles, J. I. Beitia, *Polyhedron* **1995**, *14*, 2863−2869.

[46] The ready formation of the $\{Mo_2O_4\}^{2+}$ fragment in the alcohol/pyridine medium is followed by the aggregation of two, three, four or six dimers into tetra-, penta-, hexa-, deca- or dodecanuclear polyoxoalkoxymolybdenum(v) compounds. See also: [46a] B. Modec, J. V. Brenčič, I. Leban, *Inorg. Chem. Commun.* **1998**, *1*, 161−163. [46b] B. Modec, J. V. Brenčič, R. Rotar, L. Golič, K. Prout, *Acta Crystallogr., Sect. C* **1998**, *54*, 1573−1575. [46c] B. Modec, J. V. Brenčič, L. Golič, L. M. Daniels, *Polyhedron* **2000**, *19*, 1407−1414. [46d] B. Modec, J. V. Brenčič, L. Golič, G. Giester, *Inorg. Chim. Acta* **2000**, *307*, 32−40. [46e] B. Modec, J. V. Brenčič, J. Zubieta, P. J. Hagrman, *Inorg. Chem. Commun.* **2001**, *4*, 537−540. [46f] B. Modec, J. V. Brenčič, R. C. Finn, R. S. Rarig, J. Zubieta, *Inorg. Chim. Acta* **2001**, *322*, 113−119.

[47] It is known that *N*-methylpyridinium salts result from a nucleophilic attack of pyridine on methyl halide formed from methanol and hydrogen halide. This reaction takes place only in a strongly acidic medium. Moreover, the halogenation of alcohols proceeds more readily with tertiary and secondary al-

cohols, but not with methanol. The reaction medium in our case is not acidic, as it contains mostly pyridine.

[48] G. R. Hanson, A. A. Brunette, A. C. McDonell, K. S. Murray, A. G. Wedd, *J. Am. Chem. Soc.* **1981**, *103*, 1953−1959.

[49] Z. Otwinowski, W. Minor, *Methods Enzymol.* **1997**, *276*, 307−326.

[50] G. M. Sheldrick, *SHELXS-97* and *SHELXL-97*, Universität Göttingen, **1997**.

[51] M. J. Frisch, G. W. Trucks, H. B. Schlegel, G. E. Scuseria, M. A. Robb, J. R. Cheeseman, V. G. Zakrzevski, J. A. Montgomery, Jr., J. E. Stratmann, J. C. Burant, S. Dapprich, J. M. Millam, A. D. Daniels, K. N. Kudin, M. C. Strain, O. Farkas, J. Tomasi, V. Barone, M. Cossi, R. Cammi, B. Menucci, C. Pomelli, C. Adamo, S. Clifford, J. Ochterski, G. A. Petersson, P. Y. Ayala, Q. Cui, K. Morokuma, D. K. Malick, A. D. Rabuck, K. Raghavachari, J. B. Foresman, J. Ciolslovski, J. V. Ortiz, B. B. Stefanov, G. Liu, A. Liashenko, P. Piskorz, I. Komaromi, R. Gomperts, R. L. Martin, D. J. Fox, T. Keith, M. A. Al-Laham, C. Y. Peng, A. Nanayakkara, C. Gonzales, M. Challacombe, P. M. W. Gill, B. Johnson, W. Chen, M. W. Wong, J. L. Andres, C. Gonzales, M. Head-Gordon, E. S. Replogle, J. A. Pople, *Gaussian 98*, Revision A.5, Gaussian, Inc., Pittsburgh PA, **1998**.

Received October 16, 2003
Early View Article